Self-catalyzed GaAs nanowire growth on Si-treated GaAs(100) substrates

S. Ambrosini,[1,2,3] M. Fanetti,[1,2] V. Grillo,[4] A. Franciosi,[1,2,3] and S. Rubini[1,a)]

[1]*Istituto Officina dei Materiali CNR, Laboratorio TASC, S.S. 14, Km. 163.5, I-34149 Trieste, Italy*
[2]*Sincrotrone Trieste S.C.p.A., Elettra Laboratory, S.S. 14, Km. 163.5 I-34149 Trieste, Italy*
[3]*Dipartimento di Fisica and CENMAT, Università di Trieste, 34127 Trieste, Italy*
[4]*Centro S3, CNR-Istituto Nanoscienze, Via Campi 213A, 41125 Modena, Italy and IMEM-CNR, Parco Area delle Scienze 37/A, 43010 Parma, Italy*

Self-catalyzed GaAs nanowire growth was obtained by molecular beam epitaxy on GaAs(001) substrates after predeposition of subnanometer-thick Si layers. Two substrate preparation methods are presented, the first based on the epitaxial growth of Si on GaAs and subsequent exposure to atmosphere, and the second on the direct deposition of Si on epiready GaAs substrates. X-ray photoemission spectroscopy shows that both methods result in a thin Si oxide layer that promotes the growth of GaAs nanowires aligned along the $\langle 111 \rangle$ direction. High densities of nanowires were obtained at substrate temperatures between 620 and 680 °C. Systematic electron microscopy studies indicate that nanowire growth is associated with the formation of Ga nanoparticles on the substrate surface, which act as a catalyst in the vapor-liquid-solid growth mechanism frame. The majority of the nanowires have a pure zinc-blende structure, and their photoluminescence is dominated by a photoluminescence peak 3 to 5 meV in width and centered at 1.516 to 1517 eV. © *2011 American Institute of Physics*. [doi:10.1063/1.3579449]

I. INTRODUCTION

Semiconductor nanowires (NWs) may represent important building blocks of future nanoelectronic devices. The ability to control one-dimensional growth on the nanometer scale offers unique opportunities for manipulating properties, combining materials, and designing novel devices.[1] Prototypes of nanowire-based optoelectronic devices such as photodetectors, chemical and gas sensors, waveguides, light-emitting diodes, microcavity lasers, solar cells, and nonlinear optical converters have been demonstrated.[2]

III-V NW growth via molecular-beam epitaxy (MBE) is mostly obtained by catalyst-assisted methods, wherein metal nanoparticles dispersed on the substrate surface catalyze one-dimensional semiconductor growth. The growth process has been described through the vapor-liquid-solid (VLS) model,[3,4] and gold is the most commonly utilized nanoparticle catalyst. An alternative to catalyst-assisted growth is selected area epitaxy (SAE).[5] This method for III-V semiconductor NW fabrication exploits the difference in the sticking coefficients of Ga and As on GaAs and on SiO$_2$ surfaces to restrict the growth to specific substrate areas, which are opened by lithography in a SiO$_2$ mask on the GaAs substrate.[6,7]

Both types of methods have potential drawbacks, such as substrate contamination in SAE and catalyst incorporation within the growing NWs in VLS-based methods.[8,9]

Recent interest has been raised by protocols in which group-III metals are used as catalysts for III-As NW fabrication, often also referred to as catalyst-free or self-catalyzed NW growth. A necessary element for the such growth on III-As substrates is the presence of a thin layer of oxidized Si on the substrate.[10–14] For GaAs NW growth, GaAs substrates were coated with a sputtered SiO$_2$ layer 6 to 30 nm in thickness and dipped in HF aqueous solution before being loaded in the MBE system.[11–13] In the case of InAs, a SiO$_x$ ($x \approx 1$) layer 1.3 nm in thickness was evaporated on the InAs substrates.[10,14] Very recently, catalyst-free GaAs NW growth on Si has been obtained via MBE.[15–19] In most cases,[15–18] the authors reported the presence of native oxides on the substrate surface prior to NW growth.

In this paper, we present two simple methods to obtain self-catalyzed GaAs NWs on GaAs(001) surfaces avoiding *ex situ* deposition of oxides and lithographic processes. The GaAs substrates are prepared (i) by epitaxially depositing a subnanometer-thick Si layer and oxidizing it by exposure to air or (ii) by depositing Si directly on commercial GaAs substrates, without any further processing. Both methods result in the formation of a thin Si oxide layer, as demonstrated by x-ray photoemission spectroscopy. The subsequent solid-source MBE growth yields NWs of high structural and optical quality.

II. EXPERIMENTAL DETAILS

GaAs NWs were fabricated by solid-source MBE on n-type GaAs(001) wafers in an ultrahigh-vacuum (UHV) MBE facility that includes a chamber for III-V semiconductor epitaxy and an analysis chamber for *in situ* monochromatic x-ray photoemission spectroscopy (XPS).

Two alternate approaches were used for substrate preparation. In the first approach, which we will call *epitaxial*, following thermal desorption of the native oxide at 580 °C, n-type (Si doped, N$_D = 1 \times 10^{16}$ cm^{-3}) GaAs buffer layers 0.3 μm in thickness were grown at 600 °C at a growth rate of

a)Author to whom correspondence should be addressed. Electronic mail: rubini@tasc.infm.it.

1 μm/h with a Ga to As equivalent beam pressure ratio of 10 to 12, as determined by means of an ion gauge positioned at the sample location. After the GaAs buffer growth, the sample temperature was lowered to 500 °C, and a Si layer four monolayers (MLs) thick (1 ML $= 6.26 \times 10^{14}$ cm^{-2}) was deposited under As flux at a rate of 0.02 ML/s. These growth conditions are consistent with those used to obtain high-quality Si/GaAs superlattices.[20] The substrates were then exposed to air for 15 min at 300 °C, before being introduced again in the UHV system and degassed at 300 °C for 30 min.

In the second approach, which we will call *epiready*, epiready GaAs substrates,[21] as received by the supplier, were just degassed in UHV at 300 °C for 30 min prior to the deposition of a Si layer in the same conditions reported above for epitaxial growth. XPS analysis of the substrates after different Si deposition times (not shown) revealed that the Si equivalent thickness obtained on the epiready GaAs susbtrates was reduced by a factor of 2 as compared to the epitaxial case for similar deposition times. In the following, we quote the Si equivalent thickness (in MLs) as estimated from XPS.

The two types of substrates produced through the epitaxial and epiready approaches were characterized by means of a Surface Science Instrument SSX-100-301 XPS spectrometer using the monochromatized Al K$_\alpha$ emission line at 1486.5 eV and an overall energy resolution of 0.9 eV.

GaAs NWs were fabricated by exposing the two types of substrates to Ga and As beams simultaneously, under the same flux conditions used for the growth of the GaAs buffer. Substrate temperatures in the range of 540–720 °C were explored. Typical growth times were in the range of 30 min, but for selected growth parameters the growth process was studied by exploring deposition times ranging from 10 s to 30 min. At the desired growth time, the As- and Ga-flux were both interrupted and the sample was removed from the growth chamber.

The NW morphology was characterized by means of scanning electron microscopy (SEM) using a Zeiss SUPRA40 instrument equipped with a Shottky field emission gun (SFEG). Sample NWs were transferred to a carbon-coated copper mesh, and their structural properties were investigated by means of transmission electron microscopy (TEM) using both the high-resolution TEM (HRTEM) and the annular dark field (ADF) scanning transmission electron microscopy (STEM) methods by means of a JEOL 2200 FS instrument equipped with a SFEG emitter and operated at 200 keV with a point resolution of 0.19 nm. The ADF detection angles were in the range of 46° to 128°, which does not guarantee the high-angle limit but does enhance the contrast from defects.[22,23] In a few cases, slight off-axis conditions were used to enhance the contrast between differently twinned regions. In such conditions, the residual channeling depends on the exact orientation. Energy-dispersive spectroscopy mapping (EDS) was performed with a JEOL JED 2300T spectrometer installed on the TEM microscope.

The optical quality of the NWs was investigated by means of photoluminescence spectroscopy (PL), using an excitation wavelength of 514.5 nm from an Ar$^+$ ion laser. The sample photoluminescence was dispersed by a 1m monochromator and revealed by means of a Hamamatsu photomultiplier with a GaAs photocathode.

III. RESULTS AND DISCUSSION

A. Nanowire growth

Representative SEM images of NWs obtained after 30 min of growth at a substrate temperature of 620 °C on an epitaxial substrate with 4 MLs of Si are shown in Fig. 1. NWs were grown so that they formed at an angle of 34.5° to the substrate surface, i.e., along the $\langle 111 \rangle$ direction of the GaAs substrate. At the free end of the majority of the NWs, a spherical nanoparticle (NP) with a diameter slightly larger than that of the NW is present [see Fig. 1(c)]. No visible NW tapering can be detected in Fig. 1, but higher magnification systematic studies for these growth conditions reveal slight tapering, with the average NW diameter being 95 ± 3 nm at the tip and 107 ± 4 nm at the base. A minority of shorter and thinner NWs, with no evidence of NPs at the tip, can also be detected. The contrast in Fig. 1(a) at the interface between the substrate and the NWs indicates the presence of a polycrystalline GaAs layer 0.3 to 0.4 μm in thickness, with a rough surface that can also be appreciated in the background in Fig. 1(b). Representative SEM plan-view images of the substrate surface in the early NW growth stages at 620 °C on an epitaxial substrate with 4 MLs of Si are shown in Fig. 2.
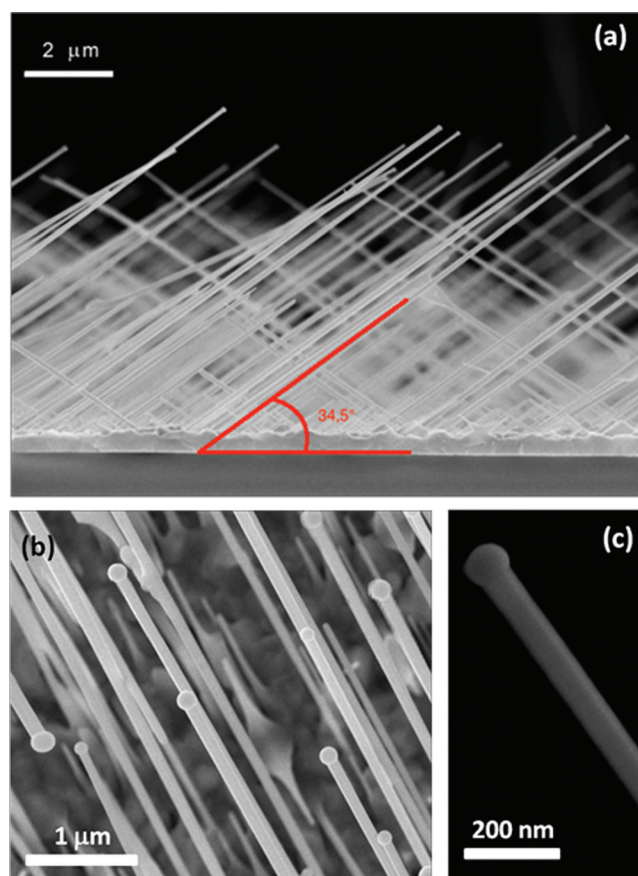

FIG. 1. (Color online) (a) Cross-sectional and (b) plan-view SEM images of representative GaAs NWs grown for 30 min at 620 °C on an epitaxial substrate with 4 MLs of Si. The 34.5° angle to the substrate surface formed by the NWs is highlighted in (a). (c) Detail of a majority NW tip.
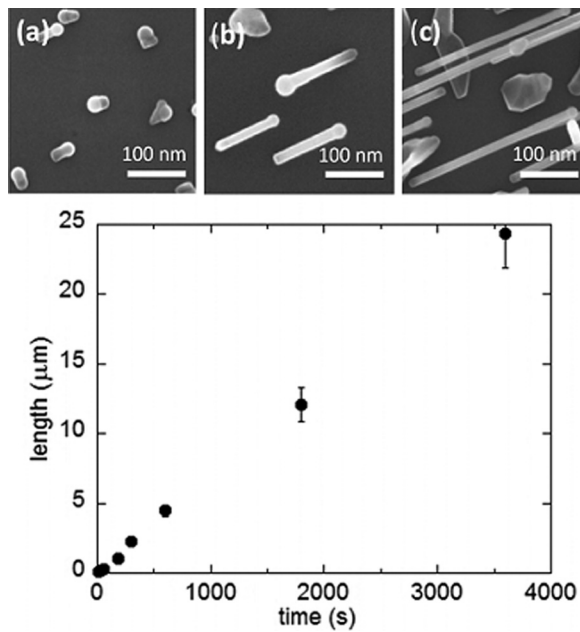
FIG. 2. Plan-view SEM images of the substrate surface after (a) 10 s, (b) 30 s, and (c) 60 s of GaAs growth at 620 °C on epitaxial substrates with 4 MLs of Si. (d) NW length as a function of growth time. The substrate temperature was 620 °C during growth.

Results for growth times of 10 s, 30 s, and 60 s are depicted in Figs. 2(a), 2(b), and 2(c), respectively. In the early NW growth stages, the condensation of GaAs appears to be related to the presence of spherical NPs on the surface. In Figs. 2(b) and 2(c), oriented one-dimensional nanostructures are seen to grow with a spherical NP at the tip. Their projection is aligned along the ⟨110⟩ substrate direction. The average lengths of the nanostructures in Figs. 2(b) and 2(c) are 150 and 260 nm, respectively, and the diameter in both cases is about 20 nm. Other three-dimensional (3D) nanostructures are occasionally observed, with a higher density after 60 s of deposition. Coalescence between such 3D formations for longer growth times is the likely origin of the rough poly-crystalline layer in Fig. 1(a).

Systematic SEM studies as a function of growth time indicate that the NW length increases linearly with time, as shown in Fig. 2(d). The measured growth rate was 6.7 nm/s (24 μm/h), i.e., far higher than the value of 1 μm/h observed for layer-by-layer growth of epitaxial GaAs in the same conditions. This confirms the importance of adatom diffusion from the substrate to the NW tip during the growth of NWs by MBE.[24,25] A linear dependence of NW length on growth time for Ga-catalyzed GaAs NWs was also reported by the authors of Ref. 12.

NW growth also was obtained on substrates prepared by the epiready method described in Sec. II. Representative plan-view SEM images of samples grown for 10 s and 30 min on epiready substrates with the equivalent of 4 MLs of Si at 620 °C are shown in Figs. 3(a) and 3(b), respectively. Also in this case, NW nucleation is associated with the presence of spherical NPs on the substrate surface. After 30 min, the majority of the NWs present a NP at the tip, while a minority of shorter and thinner NWs can be seen in the background.
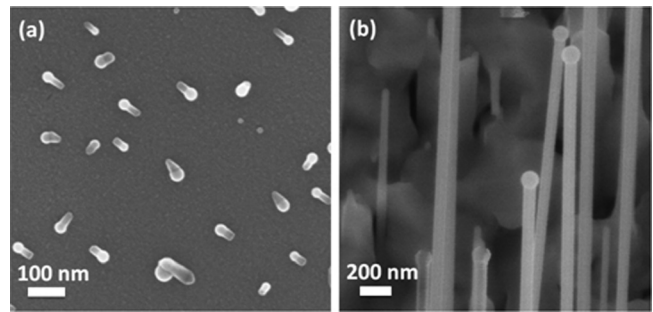

FIG. 3. Plan-view SEM images of the substrate surface after (a) 10 s and (b) 30 min of GaAs growth at 620 °C on epiready substrates with 4 MLs of Si.

The similarity of the results in Figs. 2 and 3 is quite compelling and strongly suggests that the NW nucleation mechanism is the same on the two different types of substrates. Systematic results about the dependence of the NW length on the growth time for epiready substrates (not shown) indicate a linear dependence, similar to that depicted in Fig. 2(d), further supporting our conclusion. The main result depicted in Figs. 1–3, i.e., the nucleation of NWs with spherical NPs at the tip, and their epitaxial growth in the ⟨111⟩ direction, with the length linearly increasing with time, were general features of GaAs NW growth on Si-treated substrates in all cases where NW growth was observed.

Similar results were also obtained by varying the growth temperature in a wide interval between 620 and 680 °C, with NW density and length dropping abruptly outside of this temperature interval. In Fig. 4, plan-view SEM images of the substrate surface after 30 min of growth at 580, 680, and 715 °C are shown, illustrating the strong dependence of the NW length and density on the growth temperature.

B. NW characterization

The NW structural properties were investigated for NWs grown at between 620 and 680 °C with both the epitaxial and the epiready method. No difference was found in the NW structural properties between the two cases, which will not be distinguished in what follows. Figure 5(a) shows ADF images of NWs grown at 650 °C, over a length of more than 5 μm from the NW tip. The imaging conditions were chosen in order to enhance the contrast between the twinned regions (see Sec. II). Figure 5(b) shows a HRTEM analysis of a twinned area, together with the diffractograms obtained in the two regions. HRTEM and STEM-ADF analyses revealed that the NWs have a zinc-blende (ZB) structure with no detectable stacking faults. The main structural defects observed
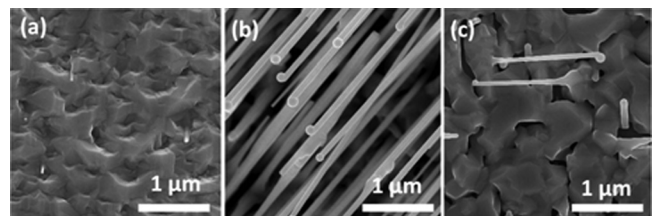

FIG. 4. Plan-view SEM images of the result of GaAs growth for 30 min on epitaxial substrates with 4 MLs of Si at different substrate temperatures: (a) 580 °C, (b) 680 °C, and (c) 715 °C.
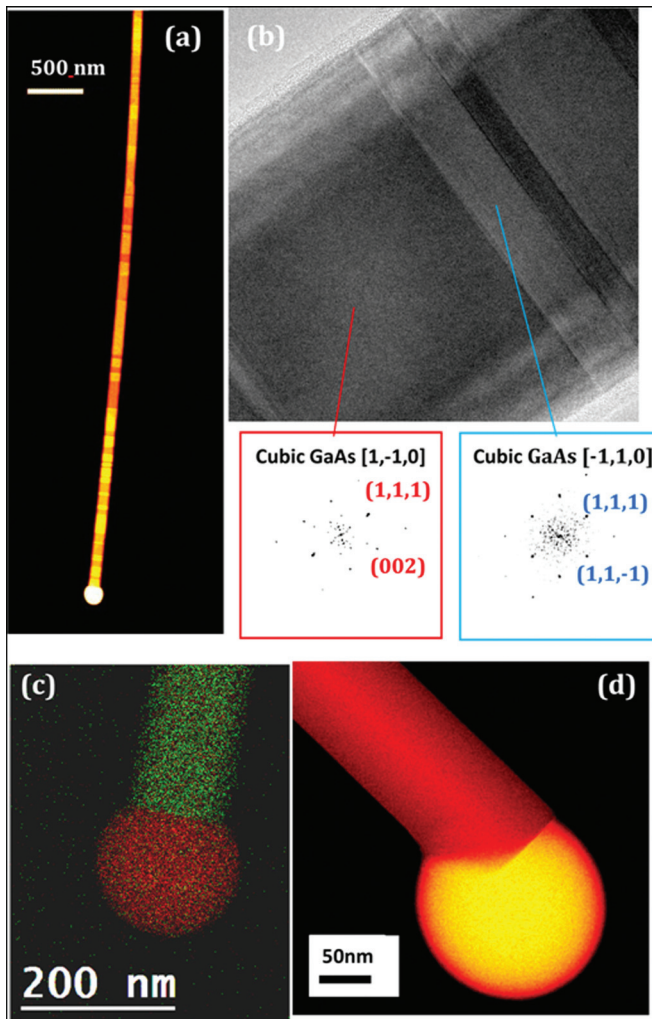
FIG. 5. (Color online) (a) ADF analysis of a GaAs NW obtained by recording images along the NW body over a length of more than 5 μm. (b) HRTEM image of a twinned region and diffractograms of the two regions indicated by the markers. (c) EDS map of a NW; dark (red) spots correspond to Ga, bright (green) to As. (d) ADF image of a NW grown at 680 °C.

were twins along the NWs. The HRTEM analysis of a twinned region in Fig. 5(b) demonstrates that no wurtzite (WZ) second phase can be found even close to the defect, and it confirms that the growth direction is $\langle 111 \rangle$.

The main result in Fig. 5, i.e., the absence of a WZ second phase within the NW body, is representative of the wide majority of the NWs grown in the range of 620–680 °C and, more specifically, of all of those exhibiting at the tip a NP larger than the NW diameter. The EDS mapping in Fig. 5(c) shows that the tip is almost completely composed of Ga, whereas As is present only in the NW body. The only difference between the NWs grown at different temperatures in the range of 620–680 °C appears to be the NP morphology and its interface with the NW body. As an example, in Fig. 5(d) we show a NW grown at 680 °C. The NP appears to partially wet the NW side, with the formation of a more complex interface.

A minority of shorter and thinner NWs, typically with diameters in the range of 20–50 nm [see Figs. 1(b) and 1(c)], exhibited no NP at the tip. In such NWs, WZ domains were detected by TEM. Examples of such NWs are shown in Fig. 6.
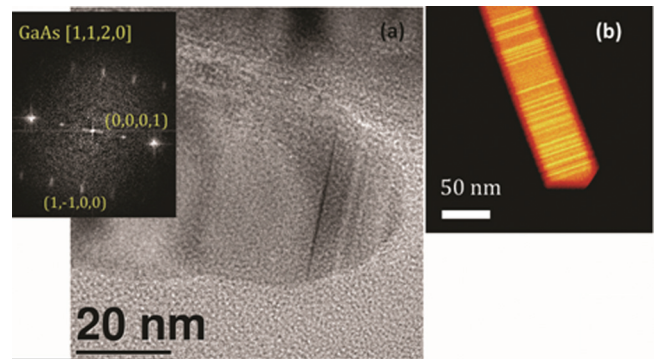

FIG. 6. (Color online) (a) HRTEM image of a minority NW. The diffractogram in the inset reveals that the tip is made of WZ GaAs. (b) Low magnification ADF-STEM image of another minority NW displaying alternate stacking of WZ and ZB regions.

Representative low temperature PL spectra of NWs grown on epiready and epitaxial Si-treated GaAs substrate are shown in Fig. 7. For comparison, the PL recorded from a sample grown for 30 min at 620 °C on an epiready substrate with 1 ML of Si is shown at the bottom of the figure. On this sample, no NWs were detected; only the background polycrystalline GaAs layer was found after growth. The PL spectra [Figs. 7(a) and 7(b)] are dominated by a very intense peak 3 to 5 meV in width, centered between 1.516 and 1.517 eV. This emission can be attributed to a zinc-blende lattice structure. The small blueshift (1 to 2 meV) relative to the GaAs free-exciton low-temperature value of 1.515 eV (Ref. 26) suggests the presence of weak quantum confinement. A weaker, modulated, broad emission feature between 1.45 and 1.5 eV can also be observed.

The comparison between spectra in Figs. 7(a)–7(c) indicates that the 1.45 to 1.5 eV broad band does not originate from the rough polycrystalline GaAs layer. Sharp PL lines in the range of 1.43–1.51 eV were observed by μ-PL in self-
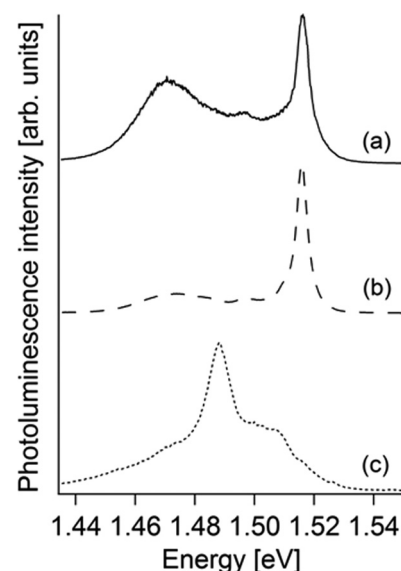

FIG. 7. Low temperature photoluminescence spectra of NWs grown for 30 min at 620 °C on (a) epiready and (b) epitaxial substrates, both with 4 MLs of Si. (c) Low temperature photoluminescence spectra of a sample grown at 620 °C on an epiready substrate with 1 ML of Si, where only the polycrystalline GaAs layer was found after 30 min of growth.

catalyzed GaAs NWs with a mixed ZB-WZ structure and were interpreted as evidence for type II band alignment in WZ-ZB heterostructures.[13] PL emission at 1.478 eV was reported for WZ self-catalyzed GaAs NWs grown on Si and was ascribed to free-exciton recombination in WZ GaAs.[27] By analogy with such results, we attribute the broad emission at 1.45 to 1.5 eV to the presence of a background of thin NWs with mixed ZB and WZ structures (see Fig. 6), with NW densities that vary from sample to sample.

C. Role of the substrate

In the preceding sections, we demonstrate efficient self-catalyzed growth of GaAs NWs on both epitaxial and epi-ready GaAs substrates treated with a Si layer 4 MLs (about 0.5 nm) thick. Despite the differences in the preparation methods, the optimal growth parameters and the resulting structural properties of the NWs are compellingly similar. In order to obtain further insight into the characteristics of the thin Si layer needed to trigger self-catalyzed growth of GaAs NWs, and specifically to clarify the nature of the Si-treated epiready substrates, we perfomed XPS analyses of the substrate surfaces before NW growth.

Results for the Ga 3p ($E_b = 104$ to 108 eV), Si 2p ($E_b \approx 100$ eV), As 3d ($E_b \approx 41$ eV), and Ga 3d ($E_b \approx 20$ eV) core level emissions are summarized in Figs. 8–10 in arbitrary units, with the binding energy E_b referred to spectrometer

Fermi level. In the analysis, the spin-orbit interaction has been explicitly taken into account for the As$_{3d}$ and Ga$_{3p}$ core level emissions by fixing the branching ratio and the energy splitting Δ_{SO} during the fit procedures [Δ_{SO} (As$_{3d}$) = 0.71 eV,[28] and Δ_{SO} (Ga$_{3p}$) = 3.45 eV, experimentally determined]. For Ga$_{3d}$ ($\Delta_{SO} = 0.43$ eV)[28] and for Si$_{2p}$ ($\Delta_{SO} = 0.6$ eV),[29] a single Voigt curve has been used.

The two topmost photoelectron energy distribution curves in Figs. 8–10 compare the core level emission from an epitaxial substrate with 4 MLs of Si (a) before and (b) after air exposure. The main spectral change following exposure to atmosphere is the complete oxidation of the Si layer, revealed by the shift toward higher binding energies of the Si 2p emission recorded at 99.94 eV in Fig. 8(a), which merges with the Ga 3p$_{5/2}$ emission in Fig. 8(b). Correspondingly, no line shape change is observed in the main, bulk-related Ga 2p and Ga 3d core emission features. We can then use the change in the relative separation between the Si 2p and Ga 3p core levels upon oxidation to estimate a Si 2p chemical shift of 2.9 eV as a result of the oxidation process, which is compatible with the suboxide state Si^{3+}.[29] Upon oxidation, the As 3d core levels display little change in the line shape of the main emission feature [see Figs. 9(a) and 9(b)], but a relatively weak emission feature appears shifted by 4.2 eV toward a higher binding energy, in agreement with the value of the As 3d chemical shift reported for As$_2$O$_5$.[30] This weak feature was observed with the same intensity in all cases of
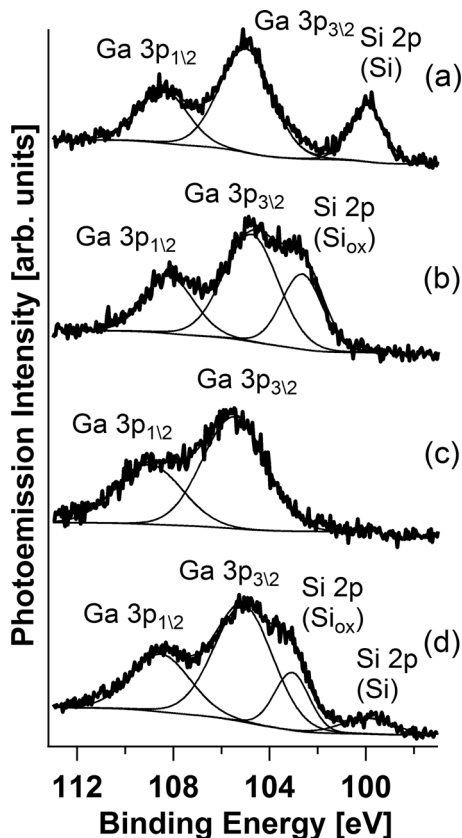

FIG. 8. Ga 3p and Si 2p core level photoemission recorded on different substrates. (a) Epitaxial substrates with 4 MLs of Si as grown and (b) after exposure to air. (c) Epiready GaAs(001) wafers as received from the supplier and (d) after deposition of 4 MLs of Si.
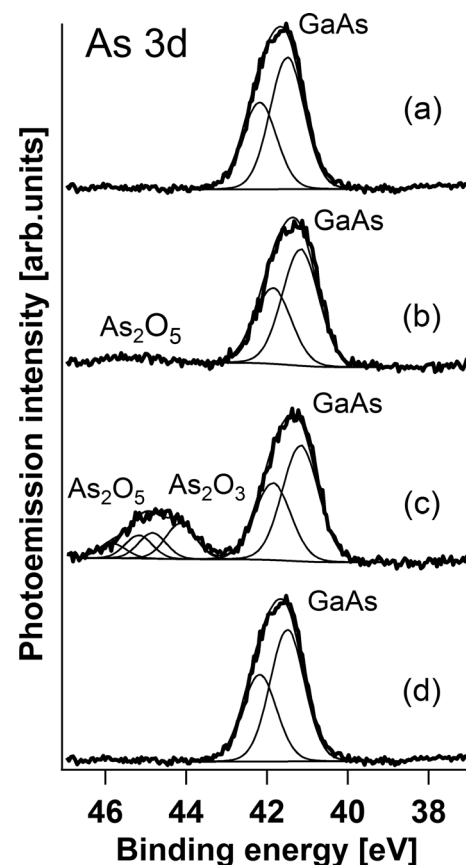

FIG. 9. As 3d core level photoemission recorded on different substrates. (a) Epitaxial substrate with 4 MLs of Si as grown and (b) after exposure to air. (c) Epiready GaAs as received from the supplier and (d) epiready substrate after deposition of 4 MLs of Si.
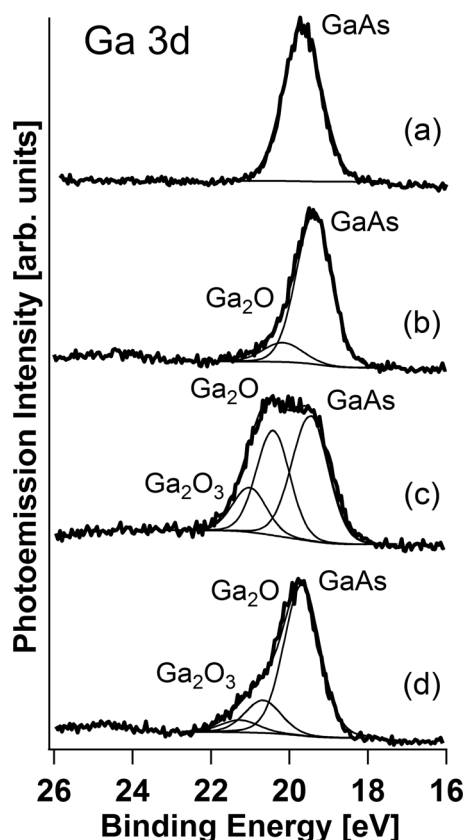
FIG. 10. Ga 3d core level photoemission recorded on different substrates. (a) Epitaxial substrate with 4 MLs of Si as grown and (b) after exposure to air. (c) Epiready GaAs as received from the supplier and (d) after deposition of 4 MLs of Si.

Si layers exposed to air, and we attribute it to the oxidation of relatively few As atoms segregating to the Si surface. We remind the reader that the Si layers were always grown under As flux. A very small new contribution is also visible in the Ga 3d emission upon oxidation, shifted by 1 eV toward higher binding energies [Fig. 10(b)]. The chemical shift is consistent with a Ga_2O configuration.[30]

The effects of Si deposition on the epiready substrates are elucidated through the analysis of the two bottommost spectra in Figs. 8–10. We can see that As oxides,[30] present on the epiready commercial substrate [Fig. 9(c)], are completely reduced by the deposition of a Si layer 4 MLs thick [see (Fig. 9(d)]. The intensity of Ga_2O and Ga_2O_3 emission[30] in Fig. 10(c) is also strongly attenuated [Fig. 10(d)]. The reduction of the native oxides of GaAs at room temperature upon deposition of Si was reported by Cuberes *et al.*[31] As a result of such a reduction, a substantial fraction of the Si layer is oxidized, but a small contribution from unreacted Si can also be detected [see Fig. 8(d)]. The presence of both the oxidized and the unreacted Si emissions allows for an estimated 3.27 eV chemical shift for Si 2p, reflecting an oxidation state close to Si^{4+}.[29]

In summary, the results of the XPS analysis in Figs. 8–10 show that both epitaxial and epiready substrates are characterized by the presence of a very thin (3 to 4 MLs) oxidized Si layer. The Si oxidation state, close to 3+ in the epitaxial case and 4+ in the epiready, does not appear to be critical for the

achievement of NW growth. Traces of Ga oxides, resulting from exposure to air, as in Fig. 10(b), or from incomplete reduction of the epiready oxide [Fig. 10(d)], do not hinder NW growth.

The presence of the Si oxide layer on GaAs is crucial to obtain NW growth instead of the deposition of an epitaxial GaAs layer. We remind the reader here that, as reported in Sec. III A, the useful growth-temperature range for self-catalyzed GaAs NWs on Si-treated substrates is between 600 and 680 °C and that the best results are obtained here at temperatures equal to or higher than 620 °C. The observed growth of NWs occurs in competition with the nucleation of 3D GaAs islands on the substrate, as can be seen in Fig. 2(c). We speculate that the selective evaporation of As,[7,32] and the reduced sticking coefficient of GaAs on the silicon oxide surface[7] at temperatures higher than 620 °C, favor the formation of Ga nanoparticles and the growth of NWs more than the deposition of a polycrystalline layer on the Si-treated substrates. The drop in NW density at temperatures higher than 680 °C can be ascribed instead to the thermal desorption of GaAs.[33]

The authors of Refs. 10, 17, and 13 proposed that openings in the Si oxide layer occurring at temperatures equal to or above 630 °C play an important role in providing nucleation sites for NW formation. Mandl *et al.*,[14] using a spectroscopic photoemission and low-energy electron microscope, observed openings appearing in a SiO_x ($x \approx 1$) layer 1.3 nm thick on InAs (111)B when heated above 600 °C. The authors attributed to the so-obtained discontinuities in the SiO_x layer the role of immobilizing In droplets in well-defined areas of the substrates, where NW nucleation will occur.

To understand whether the difference in NW density observed for growth at 580 °C and 620 °C could be related to such modifications of the substrate/oxide layer upon heating to 620 °C, growth was performed at 580 °C after prior anneals in the growth chamber throughout the temperature range of 620–650 °C. Results similar to those presented in Fig. 3(a) were obtained in all cases, i.e., low growth temperatures always led to low NW densities, irrespective of the annealing step.

Although we cannot rule out a role of temperature-dependent interactions between Ga and Si-oxide in the formation of openings in the oxide layer, the implication of our annealing experiment is that solely temperature-induced opening in the interface oxide layer cannot explain *per se* the results in Fig. 4, and that a difference in the kinetic behavior of Ga and As atoms on the substrate surface at the two temperatures must also play a role in determining the observed nucleation site density.

IV. CONCLUSIONS

We demonstrate that an ultrathin (0.5 nm) oxidized Si layer on GaAs(001) can be used to promote the growth of high-quality GaAs NWs by MBE. Such a promotion layer can be easily obtained either by exposing an epitaxial Si layer grown on GaAs to air, or by simply depositing Si on an epiready wafer and exploiting the reaction that takes

place between Si and GaAs surface oxides. This latter method, with its simplicity, appears to have great potential for the routine production of GaAs NWs, because it does not require any *ex situ* treatment before NW growth. Growth temperatures in the range of 620–680 °C yield the highest density of high-quality NWs, with NW lengths that depend linearly on the growth time. The presence of Ga nanoparticles at the tips of the NWs from the earliest stages of growth suggests a VLS-like mechanism. The majority of the NWs are purely zinc-blende, and their photoluminescence is dominated by a photoluminescence peak 3 to 5 meV wide and centered at 1.516 to 1517 eV. NWs grow in the [111] direction of the substrate, clearly demonstrating an epitaxial relationship with the substrate across the Si oxide promotion layer.

ACKNOWLEDGMENTS

[1]P. Yang, R. Yan, and M. Fardy, Nano Lett. **10**, 1529 (2010).

[2]For a recent review of nanowire-based photonic devices, see R. Yan, D. Gargas, and P. Yang, Nature Photon. **3**, 569 (2009).

[3]R. S. Wagner and W. C. Ellis, Appl. Phys. Lett. **4**, 89 (1964).

[4]B. A. Wacaser, A. D. Kimberly, J. Johansson, M. T. Borgström, K. Deppert, and L. Samuelson, Adv. Mater. **21**, 153 (2009).

[5]J. Motohisa, J. Takeda, M. Inari, J. Noborisaka, and T. Fukui, Physica E **23**, 298 (2004).

[6]J. M. Hong, S. Wang, T. Sands, J. Washburn, J. D. Flood, J. L. Merz, and T. Low, Appl. Phys. Lett. **48**, 142 (1996).

[7]D. Spirkoska, C. Colombo, M. Heiss, G. Abstreiter, and A. Fontcuberta i Morral, J. Phys.: Condens. Matter **20**, 454225 (2008).

[8]E. Carlino, F. Martelli, S. Rubini, and A. Franciosi, Philos. Mag. Lett. **86**, 261 (2006).

[9]D. E. Perea, J. E. Allen, S. J. May, B. W. Wessels, D. N. Seidman, and L. J. Lauhon, Nano Lett. **6**, 181 (2006).

[10]B. Mandl, J. Stangl, T. Mårtensson, A. Mikkelsen, J. Eriksson, L. S. Karlsson, G. Bauer, L. Samuelson, and W. Seifert, Nano Lett. **6**, 1817 (2006).

[11]A. Fontcuberta i Morral, C. Colombo, G. Abstreiter, J. Arbiol, and J. R. Morante, Appl. Phys. Lett. **92**, 063112 (2008).

[12]C. Colombo, D. Spirkoska, M. Frimmer, G. Abstreiter, J. Arbiol, and A. Fontcuberta i Morral, Phys. Rev. B **77**, 155326 (2008).

[13]D. Spirkovska, J. Arbiol, A. Gustavson, S. Conesa-Boj, F. Glas, I. Zardo, M. Heigoldt, M. H. Gass, A. L. Bleloch, S. Estrade, M. Kaniber, J. Rossler, F. Peiro, J. R. Morante, G. Abstreiter, L. Samuelson, and A. Fontcuberta i Morral, Phys. Rev. B **80**, 245325 (2009).

[14]B. Mandl, J. Stangl, E. Hilner, A. A. Zakharov, K. Hillerich, A. W. Dey, L. Samuelson, G. Bauer, K. Deppert, and A. Mikkelsen, Nano Lett. **10**, 4443 (2010).

[15]F. Jabeen, V. Grillo, S. Rubini, and F. Martelli, Nanotechnology **19**, 275711 (2008).

[16]J. H. Paek, T. Nishiwaki, M. Yamaguchi, and N. Sawaki, Phys. Status Solidi C **6**, 1436 (2009).

[17]G. E. Cirlin, V. G. Dubrovskii, Y. B. Samsonenko, A. D. Bouravleuv, K. Durose, Y. Y. Proskuryakov, B. Mendes, L. Bowen, M. A. Kaliteevski, R. A. Abram, and D. Zeze, Phys. Rev. B **82**, 035302 (2010).

[18]P. Krogstrup, R. Popovitz-Biro, E. Johnson, M. H. Madsen, J. Nygård, and H. Shtrikman, Nano Lett. **10**, 4475 (2010).

[19]S. Plissard, K. A. Dick, G. Larrieu, S. Godey, A. Addad, X. Wallart, and P. Caroff, Nanotechnology **31**, 385602 (2010).

[20]L. Sorba, G. Bratina, A. Franciosi, L. Tapfer, G. Scamarcio, B. Spagnolo, A. Migliori, P. G. Merli, and E. Molinari, J. Cryst. Growth **127**, 121 (1993).

[21]D. A. Allwood, I. R. Grant, N. J. Mason, R. A. Palmer, and J. P. Walker, J. Cryst. Growth **221**, 160 (2000).

[22]Z. Yu, D. A. Mueller, and J. Silcox, J. Appl. Phys. **95**, 3362 (2003).

[23]V. Grillo and F. Rossi, J. Cryst. Growth **318**, 1151 (2011).

[24]V. G. Dubrovskii, G. E. Cirlin, I. P. Soshnikov, A. A. Tonkikh, N. V. Sibirev, Y. B. Samsonenko, and V. M Ustinov, Phys. Rev B **71**, 205325 (2005).

[25]E. De Jong, R. R. Lapierre, and J. Z. Wen, Nanotechnology **21**, 045602 (2010).

[26]D. D. Sell, Phys. Rev. B **6**, 3750 (1972).

[27]B. V. Novikov, S. Yu. Serov, N. G. Filosofov, I. V. Shtrom, V. G. Talalaev, O. F. Vyvenko, E. V. Ubyivovk, Yu. B. Samsonenko, A. D. Bouravleuv, I. P. Soshnikov, N. V. Sibirev, G. E. Cirlin, and V. G. Dubrovskii, Phys. Status Solidi (RRL) **4**, 175 (2010).

[28]E. A. Kraut, R. W. Grant, J. R. Waldrop, and S. P. Kowalczyk, Phys Rev. B **28**, 1965 (1983).

[29]F. Jolly, F. Rochet, G. Dufour, C. Grupp, and A. Taleb-Ibrahimi, J. Non-Cryst. Solids **280**, 150 (2001).

[30]C. C. Surdu-Bob, S. O. Saied, and J. L. Sullivan, Appl. Surf. Sci. **183**, 126 (2001).

[31]M. T. Cuberes and J. L. Sacedon, Appl. Phys. Lett. **57**, 2794 (1990).

[32]C. Chatillon and D. Chatain, J. Cryst. Growth **151**, 91 (1995).

[33]Th. Hackbarth, H. Muessig, G. Jonsson, and H. Brugger, in *Proceedings of the NATO Advanced Research Workshop on Low Dimensional Structures Prepared by Epitaxial Growth or Regrowth on Patterned Substrates*, edited by K. Eberle, P. M. Petroff, and P. Demeester (Kluwer Academic, Dordrecht, 1995), pp. 345–356.